



Article

Impact of Climate Change on Water Resources in the Western Route Areas of the South-to-North Water Diversion Project

Zhongrui Ning^{1,2,3,4} , Jianyun Zhang^{1,2,3,4}, Shanshui Yuan² and Guoqing Wang^{1,2,3,4,*} 

¹ State Key Laboratory of Hydrology-Water Resources and Hydraulic Engineering, Hohai University, Nanjing 210098, China; hhunzr@hhu.edu.cn (Z.N.); jyzhang@nhri.cn (J.Z.)

² Yangtze Institute for Conservation and Development, Nanjing 210098, China; yuanshanshui@hhu.edu.cn

³ Research Center for Climate Change, Ministry of Water Resources, Nanjing 210029, China

⁴ State Key Laboratory of Hydrology-Water Resources and Hydraulic Engineering, Nanjing Hydraulic Research Institute, Nanjing 210029, China

* Correspondence: gqwang@nhri.cn

Abstract: The South-to-North Water Diversion Project (SNWDP) is a national strategic project for water shortages in northern China. Climate change will affect the availability of water resources in both source and receiving areas. A grid-based RCCC-WBM model based on climate projections from nine Global Climate Models under SSP2-4.5 was used for analyzing the changes in temperature, precipitation, and streamflow in the near future (2025–2045, NF) and far future (2040–2060, FF) relative to the baseline (1956–2000). The results showed that: (1) the temperature of the western route will increase significantly in the NF and FF with an extent of 1.6 °C and 2.0 °C, respectively, (2) precipitation will very likely increase even though Global Climate Model (GCM) projections are quite dispersed and uncertain, and (3) over half of the GCMs projected that streamflow of receiving area will slightly increase with a rate of 1.68% [−8.67%, 12.3%] and 2.78% [−3.30%, 11.0%] in the NF and FF, respectively. Climate change will support the planning of the western route to a certain extent. However, water supply risk induced by the extreme situation of climate change should be paid adequate consideration when the project operates in practice due to the large dispersion and uncertainty of GCM projections.

Keywords: South-to-North Water Diversion Project; water resources; climate change; GCMs projections



Citation: Ning, Z.; Zhang, J.; Yuan, S.; Wang, G. Impact of Climate Change on Water Resources in the Western Route Areas of the South-to-North Water Diversion Project. *Atmosphere* **2022**, *13*, 799. <https://doi.org/10.3390/atmos13050799>

Academic Editor: Ognjen Bonacci

Received: 28 March 2022

Accepted: 11 May 2022

Published: 13 May 2022

Publisher's Note: MDPI stays neutral with regard to jurisdictional claims in published maps and institutional affiliations.



Copyright: © 2022 by the authors. Licensee MDPI, Basel, Switzerland. This article is an open access article distributed under the terms and conditions of the Creative Commons Attribution (CC BY) license (<https://creativecommons.org/licenses/by/4.0/>).

1. Introduction

Distribution of annual precipitation in China presents a broad and significant characteristic of the northwest to southeast gradient [1], with more than 1103 mm in the Yangtze River [2] basin and only 466 mm, 883 mm, and 535 mm in the Yellow River [3], Huai River [4], and Hai River [5], respectively. However, the Huang-Huai-Hai plain is an important commercial grain production base, accounting for 24.2% of China's population and one-quarter of its arable land and gross domestic product [6–8]. Due to the large population, China suffers from a serious water shortage and only one third of the world average per capita water quantity [8,9]. The lack of water resources has become an important issue, affecting the development of industrial and agricultural production and urbanization [3]. The SNWDP was approved by the Ministry of Water Resources (MWR) in 2002 is a national strategic project designed to relieve the water shortages in north China [10,11].

Three routes were projected for the SNWDP: the eastern route transferred water from Jiangdu to downstream of the Huai River, the Shandong Peninsula, and Hebei Province [12]; the middle route channeled water from Danjiangkou Reservoir to Beijing and Tianjin [13]; while the design of western route plans to replenish the water resources of the upper Yellow River by diverting water from upper Yangtze River [14]. The whole SNWDP planned to transfer water from Yangtze River to Huang-Huai-Hai region via three routes with a total quantity of 14 billion km³ of water per year [15–18]. By the end of 2021, the first phase of

eastern and middle route of SNWDP had brought 49.4 billion km³ water to northern China, which equivalent to 5% of the annual streamflow of the Yangtze River basin or 80% of the annual runoff of the Yellow River basin [19].

Climate change affects the water cycle by changing the spatial and temporal pattern of temperature, precipitation, and evapotranspiration; at the same time, the water resources department is the most vulnerable department which decided the plan and operation of western line directly [8,20,21]. Rising temperatures increase the evaporation in the catchment, and the change in precipitation affects the river streamflow [22,23]. The effects of future climate change on changes in water resources in the western route of SNWDP source area and receiving area are a major focus of previous studies [12,24]. Previous studies reported that streamflow in upper Yangtze River presented an increasing trend [25] and that of the Yellow River basin no doubt showed a decreasing trend in all parts, mainly because of climate change and the large amount of human activities such as water intake in upstream and downstream, respectively [26–30]. At the same time, the results concluded by Liu [15] and Qiao [31] showed that the streamflow in Danjiangkou reservoir have decreased since the 1980s, and climate change contributed more than 80% of the change, mainly due to mainly the decrease in precipitation. The water diversion of the middle route is about ten times than that of the eastern route. In the context of climate change, the construction of the western route has become more necessary due to the decrease in water availability in the middle route and the increase in water shortages in the Yellow River basin.

The Global Climate Models (GCMs) developed by the World Climate Change Research Program (WCRP) are effective tools for predicting future climate change [32,33]. The Coupled Model Intercomparison Projects 6 (CMIP6) is the largest plan proposed by WCRP and has the largest number of participating models and the most complete design of scientific experiments and the largest simulated data [34]. Zhu et al. [35] analyzed the climate predictions of China when global warming was 1.5 °C, 2 °C, and 3 °C higher than the baseline period based on the CMIP6 simulations, and compared them with CMIP5. The evaluation showed that the GCMs in CMIP6 worked better than those in CMIP5, especially in simulating extreme precipitation.

It is a mature and widely used method to predict future streamflow and water availability by using outputs from GCMs to drive regional hydrological models [36,37]. Bao et al. [38] predicted the trend of streamflow in Hai River basin in the future by combining the variable infiltration capacity (VIC) model with climate outputs of CMIP5. The prediction showed that there might be an increasing trend for the streamflow and the increasing trend for streamflow in the north basin is higher than that in the south part. Zhang et al. [39] used the Soil and Water Assessment Tool (SWAT) model to assess the change of hydrological components for the near future period of 2013–2042 under three emission scenarios A1B, A2, and B1, and reported an increasing trend in the future streamflow at Tangnaihui gauge under A1B and B1, while the A2 scenario is characterized by a declining trend. Wang et al. [40] evaluated the potential impacts of future climate change on the hydrological regimes in upper Yangtze River basin by using eight GCMs scenarios and VIC model. The results indicated that relative to the baseline period, mean annual runoff (MAR) is projected to slightly decrease by 7.84% to 9.81% in the middle term due to rises in temperature. Su et al. [41] conducted an assessment of impact of climate change on streamflow in the upper Yangtze River basin and found that the annual streamflow will increase in most cases by the end of the 21st century. Although some studies showed that the upper Yangtze River will probably receive more precipitation and generate more streamflow in the future [42–44], there are still some studies against the findings and indicated that streamflow might decrease in the future and the reduction mainly occurs in the wet season [24,45]. Therefore, the uncertainty associated with the projection in runoff cannot be neglected [41].

The Chinese government launched planning of the great ambitious water diversion project sixty years ago. The east and middle routs were implemented and have been operating several years ago. However, only the west route is still in the planning stage. It is very necessary to study and understand the impact of climate change on the future

water availability in the water source and receiving areas of the western route to support the planning and operation of the western route. Most of previous studies mainly focused on individual sub-basins within the water source and receiving area. There are a few studies focused on the overall changes of water availability in source areas and reception areas of the western route. In this study, we drive the grid-based RCCC-WBM model by using climate projections from nine Global Climate Models under SSP2-4.5 and investigate changes of temperature, precipitation, and streamflow over the water source and reception areas in the near future (2025–2045, NF) and far future (2040–2060, FF) relative to the baseline (1956–2000). The results will support the second phase revisions of the project.

2. Materials and Methods

2.1. Study Area

Based on the project's plans, the western line will transfer water from the upper Yangtze River (YAR) to the upper Yellow River (YER). The main sourcing area covers three hydrological stations—the Batang, Yajiang, and Dajin stations with their catchment area—and the receiving area is the holistic YER. In the study, the three basins of the water diversion area were considered as one basin for calculation. The sourcing area, which contains the upper reach of Yangtze River, Ya-lung River, and Jialing River, is located in the Qinghai–Tibet Plateau covering 287,410 km² or 15.9% of the total YAR basin. The water resources of the upper YAR account for almost 40% and 15% of the total basin and China, respectively [40]. The YER basin is located within a domain 32°–42° N and 96°–119° E in northern China, with a total length of 5464 km, and a drainage area of 758,000 km². The characteristics of monsoons are prevalent in the YER with mean annual precipitation of 450 mm, of which 80% concentrates between May and September, with a maximum of over 800 mm in the southeast and a minimum of less than 150 mm in the northwest. The mean annual temperature is 5.9 °C. The lowest temperature (−8.25 °C) occurs in January while the highest (18.4 °C) can be found in July. The river basin is an important grain-producing area in China, encompassing large irrigation projects such as the Hetao irrigation area. It contains 15% of the country's cultivated land and 12% of its population [3]. Therefore, the relationship between supply and demand of water resources is very tight. The water source areas and receiving areas of the western line, the major river system of the YAR and YER, and the locations hydrological stations controlling water source and receiving areas are shown in Figure 1.

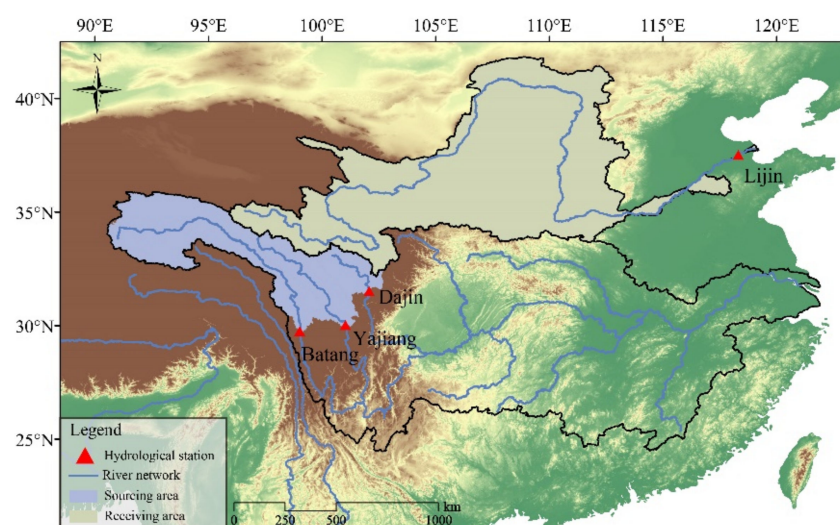


Figure 1. Water source areas, receiving area, river system, and key hydrological stations of the western line of the SNWDP.

2.2. Hydrological Model

The study uses the RCCC-WBM model for climate change assessment. The model is based on the theory of water balance and was developed by the research center of climate change. Three streamflow components—surface streamflow, groundwater, and snowmelt flow—were considered along with the processes of rainfall, snowfall, and snowmelt in the catchment. This model is a simplified large-scale conceptual hydrological model with mechanisms of streamflow generation [46]. There are four parameters in the model and the inputs include monthly precipitation, temperature, and potential evaporation. Compared with the well-known hydrological models such as the Xinanjiang model, SWAT, VIC, etc., this simple model has the advantages of being easier to understand, with fewer model parameters and more feasible transferability to poorly gauged areas [21]. The model has been applied to hundreds of catchments worldwide [47], and the structure is shown in Figure 2.

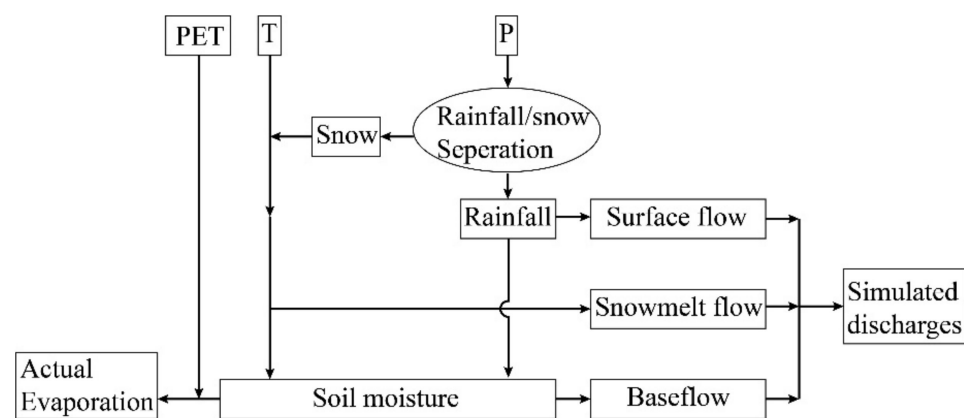


Figure 2. Structure of RCCC-WBM model.

We use threshold temperatures to distinguish between solid and liquid precipitation [48]. When T is lower than TL (-4 °C), all precipitation is assumed to be solid, and when T is greater than TH (4 °C), all precipitation is assumed to be liquid.

$$P_{SN} = \frac{TH - T}{TH - TL} P \quad (1)$$

where P is the total observed precipitation and P_{SN} represents the solid snowfall. Rainfall and snowfall are used to calculate the surface flow and snowmelt flow, while the surface flow is a function of precipitation and soil moisture. Lastly, baseflow is simulated based on the linear reservoir method.

The four parameters for the RCCC-WBM model are listed in Table 1.

Table 1. Parameters for RCCC-WBM model.

Parameters	Description	Unit	Prior Range
K_s	Surface flow coefficient	-	(0, 1)
K_g	Baseflow coefficient	-	(0, 1)
K_{sn}	Snowmelt flow coefficient	-	(0, 1)
S_{max}	Maximum soil moisture store	mm	(0, 400)

NSE (Nash–Sutcliffe) and RE (relative error) were used to assess the calibration performance of the simulated streamflow to the observed streamflow.

Considering the spatiotemporal heterogeneity of hydro-meteorological elements and underlying conditions in the study basins, simulation results obtained by a traditional lumped model may be inaccurate. Therefore, we developed a grid-based distributed model

based on the RCCC-WBM model with a resolution of 0.5° and covering the entire YAR basin and YER basin. The model was used to calculate the monthly streamflow in each grid cell and routing scheme in the VIC (variable infiltration capacity) model was referenced in the model flow concentrating to outlet of study area [11,48].

2.3. Data Sources

Daily gridded meteorological data around China with a resolution of 0.25° and a time span from 1961–2018 [49–51] were collected. The data were converted to a resolution of 0.5° using the cubic convolution interpolation method in order to drive the hydrological model. We also collected daily observed streamflow data at 4 hydrological stations from the Hydrological Yearbook of the MWR.

The SNWDP was designed based on the historical streamflow from 1956 to 2000. Therefore, we took this period as the baseline, and defined 2026 to 2045 as the near future (NF) and 2041 to 2060 as the far future (FF).

We used SSP2-4.5 scenarios to drive GCM for climate prediction because the low emission scenario (SSP1-2.6) and high emission scenarios (SSP4-6.0 and SSP5-8.5) were usually considered as extreme emission conditions with higher uncertainty [40,41], while the medium emission scenario (SSP2-4.5) has the highest possibility of occurring in the future. However, due to differences in simulation mechanisms, initial conditions, parameterization schemes, spatial resolutions, and so on, the performances of GCMs in different regions are quite different [52,53]. Some scholars have evaluated the applicability of different GCMs in China and the YER basin [54–56]. The results showed that some models, such as BCC-CSM2, worked better than others. Therefore, we selected 9 GCMs (Table 2) that have better performances for the followed analyses. Climate projections from 9 GCMs under SSP2-4.5 were downloaded from <https://www.wcrp-climate.org/wgcm-cmip/wgcm-cmip6> (accessed on 11 March 2022) with the time series ranging from 1901 to 2099. Additionally, the outputs from GCMs were downscaled to 0.5° grids using the statistical downscaling model (LARS-WG) and the bias was corrected by referring to gridded meteorological data in order to match the resolution and drive the grid-based RCCC-WBM model for streamflow prediction [57].

Table 2. General information of the 9 GCMs used in this study.

Nos.	GCMs	Country and Developer	Resolution	Nos.	GCMs	Country and Developer	Resolution
1	BCC-CSM2	China, BCC	$1.25^\circ \times 1.25^\circ$	6	FIO-ESM	China, FIO	$2.8^\circ \times 2.8^\circ$
2	CNRM-CM6	France, CNRM-CERFACS	$1.4^\circ \times 1.4^\circ$	7	GFDL-ESM4	America, GFDL	$1.25^\circ \times 1^\circ$
3	CSIRO-MK-3	Australia, CSIRO	$1.9^\circ \times 1.9^\circ$	8	GISS-E2-H	America, GISS	$2.0^\circ \times 2.5^\circ$
4	FGOALS-G3	China, LASG-CES	$2.0^\circ \times 2.25^\circ$	9	MIROC-ES2L	Japan, CCSR/NIES/FRCGC	$2.8^\circ \times 2.8^\circ$
5	CCSM4	America, NCAR	$1.25^\circ \times 0.9^\circ$				

3. Results

3.1. Model Calibration

A qualified hydrological model is an important precondition for streamflow simulations. Within the source area and receiving area of the western route, there are monthly observed streamflow data available at four control hydrological stations and the length of the data series is over 30 years. A driving grid RCCC-WBM model using meteorological data for streamflow simulation and the results are given in Table 3 and Figure 3.

Table 3. Statistics of streamflow simulation results for the five hydrometric stations within source areas of the South-to-North Water Diversion Project.

Areas	Stations	Model Calibration			Model Validation		
		Data Series	NSE(%)	Re(%)	Data Series	NSE(%)	Re(%)
Source area	Dajin	1957–1989	83.7	−1.1	1990–2000	85.1	−0.2
	Yajiang	1956–1989	86.6	−1.9	1990–2000	89.3	2.1
	Batang	1960–1989	83.3	0.4	1990–2000	74.6	−0.7
Receiving area	Lijin	1956–1989	80.6	1.5	1990–2000	76.2	0.4

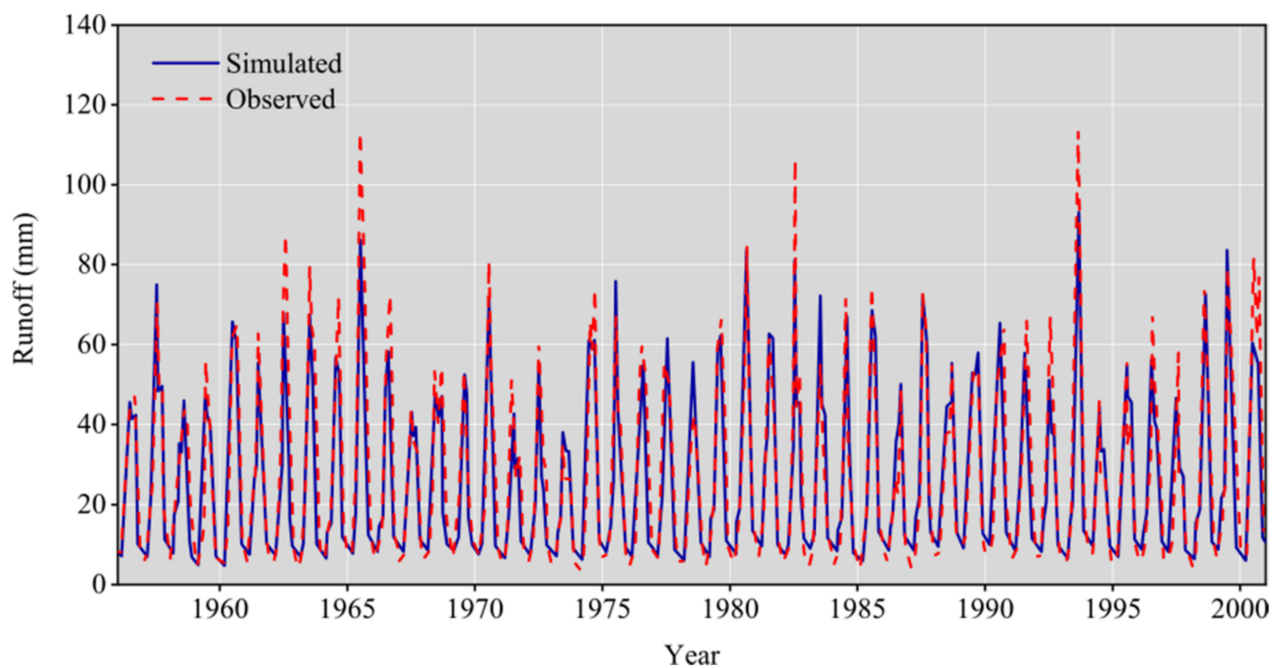
**Figure 3.** Simulated and recorded streamflow series in the Yajiang station.

Table 3 showed that the grid-based RCCC-WBM performed well for simulating streamflow for four hydrological stations, the NSE in both the calibration stage and validation stage was higher than 70%, and the absolute value of RE for simulated streamflow and observed values was lower than 2%. The time series of streamflow in Figure 3 illustrates that the simulated streamflow fit the shape of the recorded value well, and the peak and valley values were close to those recorded. Combining the results of Table 3 and Figure 3, the grid-based RCCC-WBM could describe the hydrological process in the catchment well and could be used to assess the streamflow for future climate change scenarios.

3.2. Changes in Temperature and Precipitation in Western Route

Using meteorological data from nine GCMs, the time series of temperature and precipitation for the western route source area (WRSa) and receiving area (WRRa) are shown in Figure 4.

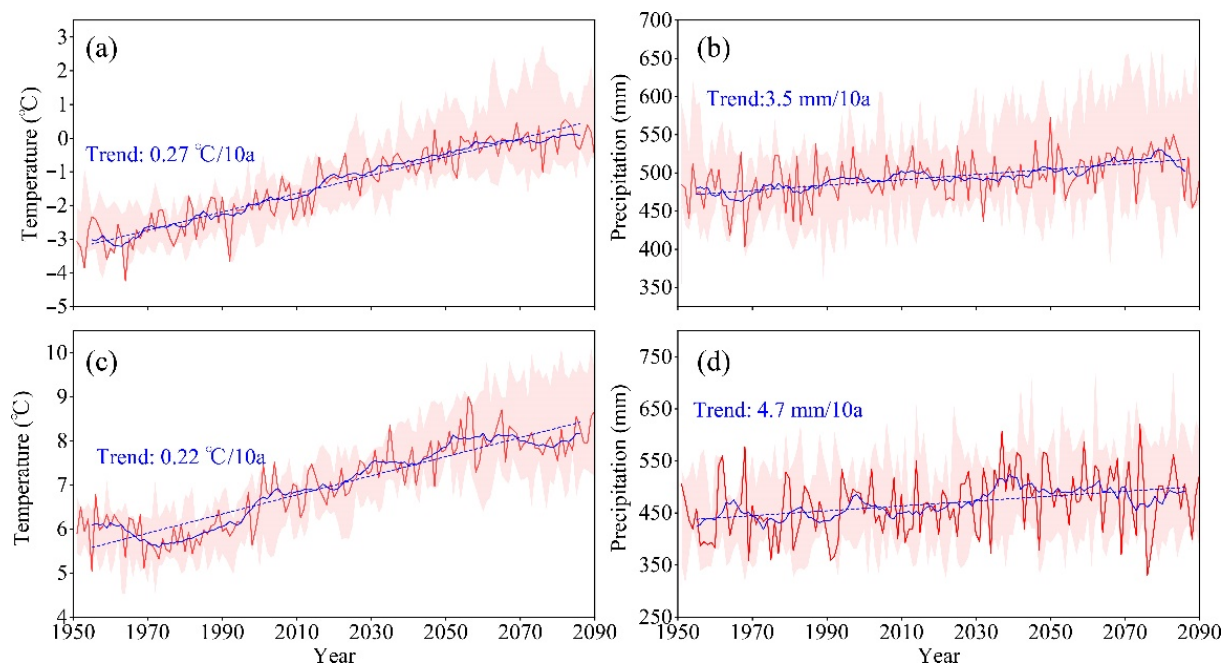


Figure 4. Temperature (left) and precipitation (right) series of 9 GCMs (red shadow) during 1951–2080 in WRSA (a,b) and WRRR (c,d). Red and blue solid line present the middle condition among 9 GCMs and corresponding 10-year moving averages, respectively; blue dotted lines display the linear trend of the moving windows.

Figure 4 shows that: (1) Temperature in the WRSA and WRRR from present to 2070 shows an upward trend, and the rising rate in the WRRR may decrease and even become negative after 2050. (2) The interdecadal characteristics of the WRRR temperature change were more obvious, with the temperature in 1970–2000 and 2070 were lower and were significantly higher in 2000–2070 than the linear trend. (3) Precipitation in the western line was likely to rise persistently with rates of 3.4 mm/10a and 4.6 mm/10a in the WRSA and WRRR, respectively. From the perspective of decadal characteristics, the precipitation in the WRSA is lower in 2015–2050, and may become more abundant after 2050, while that in the WRRR will be higher than the linear trend in 2030–2070, and may be lower after 2050.

Temperature and precipitation changes in NF and FF relative to baseline are shown in Figure 5.

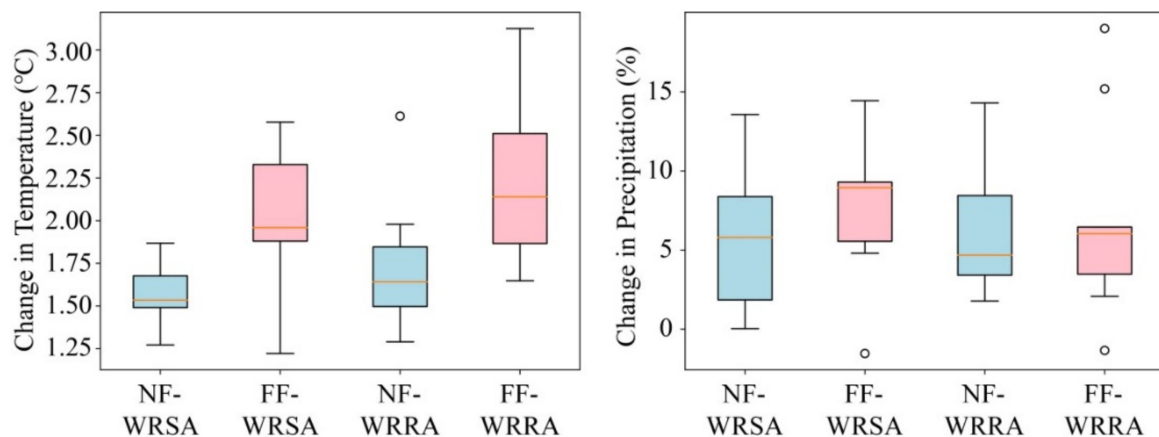


Figure 5. Change of temperature (a) and precipitation (b) in near future and far future relative to baseline for SNWDP western route.

From Figure 5a, it can be shown that: (1) all GCMs projected that the temperature will increase in NF and FF even though they are predicted to have a different rate of increase; (2) temperature will increase significantly in NF with a rate of 1.66°C and 1.57°C , respectively, with ranges of $[1.27^{\circ}\text{C}, 1.92^{\circ}\text{C}]$ and $[1.37^{\circ}\text{C}, 1.64^{\circ}\text{C}]$ in the WRSA and WRR; and (3) the temperature will rise higher in the far future than the near future. On average, the temperature will rise by 2.09°C $[1.64^{\circ}\text{C}, 3.09^{\circ}\text{C}]$ and 1.93°C $[1.82^{\circ}\text{C}, 2.64^{\circ}\text{C}]$, respectively, in the WRSA and WRR. However, the uncertainty of the temperature change in the FF is larger than that in the NF.

Figure 5b describes the near future and far future precipitation change relative to the baseline. It shows that: (1) Uncertainty in changes of precipitation were more obvious than that of temperature as a GCM may project an increase in precipitation while another one might present a decrease. However, it did not happen frequently. All the GCMs projected that precipitation will increase in the near future and far future in the western route and also expect near future changes in the WRR. (2) Precipitation will increase by 4.90% (1.43%, 14.1%) and 6.06% (2.48%, 6.72%), respectively, in NF and FF for WRSA. For the WRR, most GCMs projected that precipitation will increase by 5.35% with a range of $(-1.00\%, 12.9\%)$ in the near future and increase by 8.53% (5.32%, 13.8%) in the far future.

Temperature rise will certainly enlarge the catchment evapotranspiration under the same conditions of water supply and may finally lead to a reduction in streamflow. According to a previous study, streamflow in humid areas might decrease approximately 4% for every 1 degree centigrade rise in temperature and global mean evaporation will increase by 1–3% [23,58,59]. The changes in temperature and precipitation change the water and thermal fluxes in the basin, which will definitely affect water availability in SNWDP.

3.3. Changes in Streamflow in the Western Route

The streamflow series in the source area and receiving area from the nine GCMs in the grid-based RCCC-WBM model are shown in Figure 6.

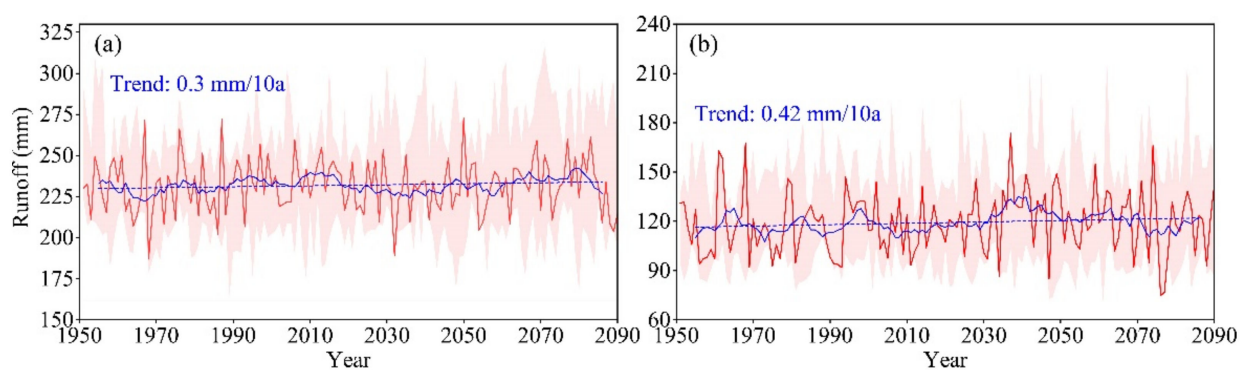


Figure 6. Streamflow series of 9 GCMs (red shadow) during 1951–2080 in WRSA (a) and WRR (b). Red line presents the middle condition among 9 GCMs. Red and blue solid line present the middle condition among 9 GCMs and corresponding 10-year moving averages, respectively; blue dotted lines display the linear trend of the moving windows.

Figure 6 shows that: (1) The streamflow in the WRSA and WRR from the present to 2080 shows a slightly upward trend with an average rate of $0.3\text{ mm}/10\text{a}$ and $0.4\text{ mm}/10\text{a}$, respectively, and (2) the change in streamflow in the source area shows similar decadal characteristics with precipitation and water resources after 2040 possibly being more abundant than in 2020–2040. The evolution of streamflow in the receiving area was also similar to that for precipitation, and after 2030 it may show an obvious downward trend. The simulation results showed that WRR streamflow will still be above the linear trend from 2030 to 2070, but will decrease significantly after 2070. Streamflow changes in the NF and FF relative to the baseline of the western route are shown in Figure 7.

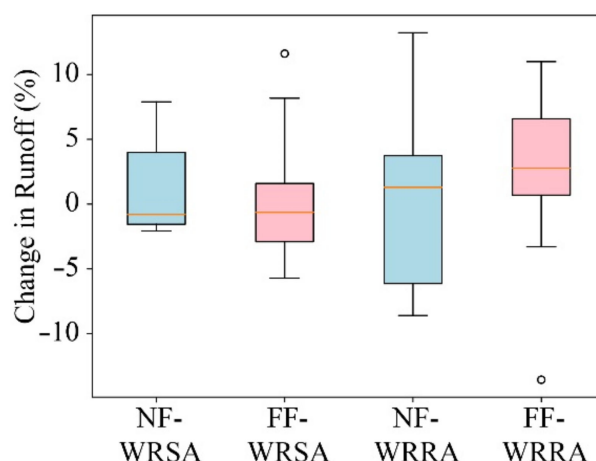


Figure 7. Change of streamflow in near future and far future relative to baseline for SNWDP western route.

Figure 7 describes the near future and far future streamflow change relative to the baseline. It shows that: (1) The change in streamflow had a higher uncertainty than that for precipitation, with about half of the GCMs projecting that streamflow in the NF and FF may increase relative to the baseline while the others showed that may decrease, and (2) for the WRSA, the GCMs predicted a change rate of streamflow of -0.80% (-2.07% , 7.89%) and -0.63% (-5.70% , 8.17%) in the near future and the far future, respectively, and for the WRRA, the change rate was 1.68% (-8.67% , 12.3%) and 2.78% (-3.30% , 11.0%), respectively.

4. Discussion

4.1. Variations of Temperature, Precipitation and Streamflow in Western Route

Climate change has been observed worldwide, with a warming temperature of $0.85\text{ }^{\circ}\text{C}$ ($0.65\text{ }^{\circ}\text{C}$ to $1.06\text{ }^{\circ}\text{C}$) over the period 1880 to 2012 [58] globally. Temperature in the areas of this study increased constantly and all the GCMs projected that it will continue to rise under the SSP2-4.5 scenario. This is consistent with previous studies [60,61]. Higher temperatures will accelerate the speed of evaporation and increase the irrigation quota [62]. The Yellow River basin, the receiving area of the South-to-North Water Diversion Project's western route, is an important irrigation district in China. According to national statistics, 91% of the water for crops was taken from the Yellow River [63]. Therefore, adequate water resources in the Yellow River basin will help to ensure food security in China [64].

The source area of the SNWDP's western route is mainly located in the upper YAR. Numerous studies indicated that the upper YAR will receive more precipitation in the future along with an increase in streamflow [41,65–68], which is consistent with the findings in this study. However, some studies such as Li [69] reported that streamflow at the head water of Zhimenda station may actually decrease by $4.6\text{ m}^3/\text{s}/10\text{a}$, which is in conflict with the conclusions of this study. The difference may be due to differences in the baseline and changing periods. At the same time, there is greater uncertainty in predicting any future streamflow when using the GCMs [70,71]. As Figure 4 shows, almost all the GCMs projected that precipitation in the future western route will increase, but CSIRO-MK3-6 projected that in the far future precipitation in the Yellow River basin will actually decrease by -1.5% . Figure 7 also shows the uncertainties in the results of the streamflow simulations.

It is noteworthy that for the WRRA, although more than half of the GCMs projected that streamflow would increase during the NF and FF, the uncertainty was much greater than that of the WRSA. CSIRO-MK3-6 predicted a decrease in WRRA streamflow of about 10% and 15% in the NF and FF, respectively. Similarly, FIO-ESM predicted a streamflow reduction of more than 5% for WRSA in the FF. Thus, the risk of streamflow reduction due to climate change needs to be taken into account during project operations.

According to the description of uncertainty by the IPCC [72], temperature in the western route source area and receiving area is virtually guaranteed to increase; precipitation is also extremely likely to increase in the NF and is very likely to increase in the FF. the projection of future streamflow change in the source area shows a large uncertainty while streamflow in the receiving area will likely increase in both periods of NF and FF, which is beneficial to the operation of the SNWDP.

4.2. Uncertainty

Many factors can lead to uncertainty in research including the outputs of the GCMs, the structure and parameters of hydrological models, and different scenarios for the future. According to the uncertainty analysis conducted by Vetter [73], the outputs of the GCMs contribute the most to the uncertainty, followed by climate models, and finally by hydrological models.

A statistical downscaling model (LARS-WG) was used in the outputs of the GCMs in order to enable a quantitative assessment of climate impacts across different regions in a consistent setting. These data were bias corrected by referring to gridded meteorological data. However, the WRSA is located in the Qinghai–Tibet Plateau (QTP) with a complicated terrain and relatively sparse observed stations, which makes it difficult to describe meteorological conditions accurately. Bao et al. [74] reported that the reanalysis dataset showed a colder and drier bias than the observed data in QTP even though the dataset captured the spatial patterns of climatic variables very well. Therefore, the preprocessing of GCMs may contribute a higher uncertainty in streamflow simulations and projections than the structure of hydrological models.

Another uncertainty in this research is linked to the calibration process of hydrological models. We used the historical series of hydro-meteorological data and SCE-UA algorithm based on maximizing the NSE and minimizing the RE criteria. Impacts of climate change were investigated under the assumption that the optimal parameters found in the calibration process would remain valid in the future. Wang et al. [47] indicated that K_s , K_g , and K_{sn} may be significantly related to a steady infiltration rate, saturated hydraulic conductivity, and latitude of the basin, respectively. These characteristics are related to the soil properties of the basin, which are fairly consistent over time [75]. However, the value of s_{max} has a close relationship with soil porosity, which may change significantly with the amount of vegetation [76]. Many studies proved that the annual average Normalized Difference Vegetation Index (NDVI) of the Yellow River Basin increased significantly from 1982 to 2016 [77,78], and such an increase was mainly due to the reforestation during the soil–water conservation practices over the past 30 years and also partially due to climate variability—especially temperature increases [79]. Therefore, the vegetation condition in the study area may change continuously in the future, which will lead to a change in hydrological model parameterization. Previous studies have shown that the uncertainties related to parameters are more significant than the effects of the model's structure in snow-dominated river basins [80]. With 22.2% and 6.5% of the streamflow is fed by snowmelt water and glacier-melt water, respectively, in upper YAR [81], the choice of model parameters might produce higher uncertainties for the projected streamflow.

4.3. Limitations

There are also some limitations in this study. The water balance model we used in the calculation ignores some factors such as glacier retreat, frozen soil degradation, and thawing of permafrost layers. Thus, the actual change of water resources may be more complicated and contain more uncertainty. Snowmelt is a dominant contributor to streamflow [82], especially for those headwater basins with elevations greater than 2000 m above mean sea level [49]. Under the influence of climate change, this proportion may continue to increase and the amount of surface water resources in the YAR basin may become more abundant. However, observed data has shown a decreasing trend of meltwater contributions to the streamflow since the later part of the twentieth century [82]. The magnitude and timing of

snowmelt has changed considerably during the period between 1979 and 2019 [48]. Due to the reduction in snow accumulation, the future snow meltwater supply may subsequently drastically decrease [83,84].

This study focused on the change of natural streamflow in the future relative to the baseline period. However, the YER basin has been affected by human activities considerably, which were not considered in this hydrological model. The projected streamflow therefore represents water yield in a natural state rather than in an actual situation with intensive human disturbance.

5. Conclusions

This study analyzed the change of temperature, precipitation, and streamflow affected by climate change in the South-to-North Water Diversion Project western route. We concluded that:

- (1) Temperature will increase by 1.66 °C [1.27 °C, 1.92 °C] and 1.57 °C [1.37 °C, 1.64 °C] during 2025–2045 relative to the baseline period (1956–2000) in the western route source area and receiving area, respectively; during the far future (2040–2060) the increase will be 2.09 °C [1.64 °C, 3.09 °C] and 1.93 °C [1.82 °C, 2.64 °C], respectively.
- (2) Precipitation will very likely increase for the western route although the GCM projections are quite dispersed and uncertain, which will be beneficial to the operation of the SNWDP.
- (3) Grid-based RCCC-WBM performs well for streamflow simulations for the study areas. The median streamflow simulations among the nine GCMs will likely increase by less than 3% relative to the baseline for the western route.
- (4) Climate change will support the planning of the western route to a certain extent; however, the risk to the water supply caused by climate change in the plan and operation of the western route still require sufficient attention.

Results of this study will support the design and operation of the SNWDP. Meanwhile, there are many other large-scale water diversion projects such as the Snow Mountain Scheme in Australia and the California State Water Project in the United States [85,86]. The effect of climate change on different aspects are complex and varied, and the research methods used in this paper can provide a reasonable idea for researchers focusing on these areas.

Author Contributions: Z.N.: data curation, formal analysis, and visualization; G.W.: conceptualization and methodology; J.Z. and S.Y.: review, discussion, and revision. All authors have read and agreed to the published version of the manuscript.

Funding: The research was supported by the National Key Research and Development Programs of China (Grant No. 2021YFC3201100), the National Natural Science Foundation of China, China (52121006, 92047301, 52079026), and the Belt and Road Fund on Water and Sustainability of the State Key Laboratory of Hydrology-Water Resources and Hydraulic Engineering, China (2020nkzd01, 2021490211).

Institutional Review Board Statement: Not applicable.

Informed Consent Statement: Not applicable.

Data Availability Statement: The data presented in this study are available on request from the corresponding author.

Acknowledgments: All authors appreciate the journal editors and anonymous reviewers for their great efforts reviewing the manuscript and their constructive comments.

Conflicts of Interest: The authors declare no conflict of interest.

References

1. Lu, Y.; Jiang, S.; Ren, L.; Zhang, L.; Wang, M.; Liu, R.; Wei, L. Spatial and Temporal Variability in Precipitation Concentration over Mainland China, 1961–2017. *Water* **2019**, *11*, 881. [\[CrossRef\]](#)
2. Shu, Z.; Zhang, J.; Jin, J.; Wang, G.; Wang, L.; Cao, M. Evolution Characters and Causes of the Dry Season Runoff for the Major Rivers in China during 1961–2018. *Adv. Clim. Chang. Res.* **2021**, *17*, 340. [\[CrossRef\]](#)
3. Wu, L.; Liu, X.; Ma, X. Spatio-Temporal Evolutions of Precipitation in the Yellow River Basin of China from 1981 to 2013. *Water Supply* **2016**, *16*, 1441–1450. [\[CrossRef\]](#)
4. Yan, D.; Han, D.; Wang, G.; Yuan, Y.; Hu, Y.; Fang, H. The Evolution Analysis of Flood and Drought in Huai River Basin of China Based on Monthly Precipitation Characteristics. *Nat. Hazards* **2014**, *73*, 849–858. [\[CrossRef\]](#)
5. Wang, G.; Zhang, J.; Li, Y.; Bao, Z.; Jin, J.; Yan, X.; Liu, C. Variation Trend of Future Climate for the Hai River Basin Based on Multiple GCMs Projections. *Resour. Sci.* **2014**, *36*, 1043–1050.
6. Ling, M.; Han, H.; Wei, X.; Lv, C. Temporal and Spatial Distributions of Precipitation on the Huang-Huai-Hai Plain during 1960–2019, China. *J. Water Clim. Chang.* **2021**, *12*, 2232–2244. [\[CrossRef\]](#)
7. Li, Y.; Xie, Z.; Qin, Y.; Zhou, S. Spatio-Temporal Variations in Precipitation on the Huang-Huai-Hai Plain from 1963 to 2012. *J. Earth Syst. Sci.* **2018**, *127*, 101. [\[CrossRef\]](#)
8. Liu, Y.; Zhang, J.; Wang, G.; Wang, G.; Jin, J.; Liu, C.; Wan, S.; He, R. How Do Natural Climate Variability, Anthropogenic Climate and Basin Underlying Surface Change Affect Streamflows? A Three-Source Attribution Framework and Application. *J. Hydro-Environ. Res.* **2020**, *28*, 57–66. [\[CrossRef\]](#)
9. CREEI. *Water Resources Assessment and Its Development & Utilization in China*; China Hydropower Press: Beijing, China, 2014.
10. Zhang, Q. The South-to-North Water Transfer Project of China: Environmental Implications and Monitoring Strategy. *J. Am. Water Resour. Assoc.* **2009**, *45*, 1238–1247. [\[CrossRef\]](#)
11. Wang, G.; Zhang, J.; Jin, J.; Pagano, T.; Bao, Z.; Liu, C.; Liu, Y.; Yan, X. Assessing Water Resources in China Using PRECIS Projections and a VIC Model. *Hydrol. Earth Syst. Sci.* **2012**, *16*, 231–240. [\[CrossRef\]](#)
12. Fang, G.; Zhu, X.; Huang, X. Risk Analysis of Floodwater Resources Utilization along Water Diversion Project: A Case Study of the Eastern Route of the South-to-North Water Diversion Project in China. *Water Supply* **2019**, *19*, 2464–2475. [\[CrossRef\]](#)
13. Han, B.; Meng, N.; Zhang, J.; Cai, W.; Wu, T.; Kong, L.; Ouyang, Z. Assessment and Management of Pressure on Water Quality Protection along the Middle Route of the South-to-North Water Diversion Project. *Sustainability* **2019**, *11*, 3087. [\[CrossRef\]](#)
14. Zhang, J.; Ma, X.; Jing, L.; Yang, L. Plan optimization of the west route of South-to-North Water Diversion Project. *South-to-North Water Transf. Water Sci. Technol.* **2020**, *18*, 109–114. [\[CrossRef\]](#)
15. Liu, X.; Liu, C.; Luo, Y.; Zhang, M.; Xia, J. Dramatic Decrease in Streamflow from the Headwater Source in the Central Route of China's Water Diversion Project: Climatic Variation or Human Influence? *J. Geophys. Res. Atmos.* **2012**, *117*, D06113. [\[CrossRef\]](#)
16. Yan, B.; Chen, L. Coincidence Probability of Precipitation for the Middle Route of South-to-North Water Transfer Project in China. *J. Hydrol.* **2013**, *499*, 19–26. [\[CrossRef\]](#)
17. Yang, S.; Xu, K.; Milliman, J.; Yang, H.; Wu, C. Decline of Yangtze River Water and Sediment Discharge: Impact from Natural and Anthropogenic Changes. *Sci. Rep.* **2015**, *5*, 12581. [\[CrossRef\]](#)
18. Yang, S.L.; Shi, B.; Fan, J.; Luo, X.; Tian, Q.; Yang, H.; Chen, S.; Zhang, Y.; Zhang, S.; Shi, X. Streamflow Decline in the Yellow River along with Socioeconomic Development: Past and Future. *Water* **2020**, *12*, 823. [\[CrossRef\]](#)
19. Yin, Y.; Wang, L.; Wang, Z.; Tang, Q.; Piao, S.; Chen, D.; Xia, J.; Conradt, T.; Liu, J.; Wada, Y. Quantifying Water Scarcity in Northern China within the Context of Climatic and Societal Changes and South-to-North Water Diversion. *Earths Future* **2020**, *8*, e2020EF001492. [\[CrossRef\]](#)
20. Wang, G.; Zhang, J.; He, R.; Liu, C.; Ma, T.; Bao, Z.; Liu, Y. Runoff Sensitivity to Climate Change for Hydro-Climatically Different Catchments in China. *Stoch. Environ. Res. Risk Assess.* **2017**, *31*, 1011–1021. [\[CrossRef\]](#)
21. Guan, X.; Zhang, J.; Elmahdi, A.; Li, X.; Liu, J.; Liu, Y.; Jin, J.; Liu, Y.; Bao, Z.; Liu, C. The Capacity of the Hydrological Modeling for Water Resource Assessment under the Changing Environment in Semi-Arid River Basins in China. *Water* **2019**, *11*, 1328. [\[CrossRef\]](#)
22. Ning, Z.; Zhang, J.; Wang, G. Variation and Global Pattern of Major Meteorological Elements during 1948–2016. *China Environ. Sci.* **2021**, *41*, 4085–4095. [\[CrossRef\]](#)
23. Shi, X.; Qin, T.; Nie, H.; Weng, B.; He, S. Changes in Major Global River Discharges Directed into the Ocean. *Int. J. Environ. Res. Public Health* **2019**, *16*, 1469. [\[CrossRef\]](#)
24. Zhang, L.; Qin, L.; Yang, Z.; Xia, J.; Zeng, S. Climate Change Impacts on Hydrological Processes in the Water Source Area of the Middle Route of the South-to-North Water Diversion Project. *Water Int.* **2012**, *37*, 564–584. [\[CrossRef\]](#)
25. Luo, Y.; Qin, N.; Zhou, B.; Li, J.; Liu, J.; Wang, C.; Pang, T. Change of Runoff in the Source Region of the Yangtze River from 1961 to 2016. *Res. Soil Water Conserv.* **2019**, *26*, 123–128. [\[CrossRef\]](#)
26. Zheng, Y.; Huang, Y.; Zhou, S.; Wang, K.; Wang, G. Effect Partition of Climate and Catchment Changes on Runoff Variation at the Headwater Region of the Yellow River Based on the Budyko Complementary Relationship. *Sci. Total Environ.* **2018**, *643*, 1166–1177. [\[CrossRef\]](#)

27. Tian, S.; Xu, M.; Jiang, E.; Wang, G.; Hu, H.; Liu, X. Temporal Variations of Runoff and Sediment Load in the Upper Yellow River, China. *J. Hydrol.* **2019**, *568*, 46–56. [\[CrossRef\]](#)
28. Wu, J.; Miao, C.; Wang, Y.; Duan, Q.; Zhang, X. Contribution Analysis of the Long-Term Changes in Seasonal Runoff on the Loess Plateau, China, Using Eight Budyko-Based Methods. *J. Hydrol.* **2017**, *545*, 263–275. [\[CrossRef\]](#)
29. Guan, X.; Zhang, J.; Bao, Z.; Liu, C.; Jin, J.; Wang, G. Past Variations and Future Projection of Runoff in Typical Basins in 10 Water Zones, China. *Sci. Total Environ.* **2021**, *798*, 149277. [\[CrossRef\]](#)
30. Wang, G.; Zhang, J.; Guan, X.; Bao, Z.; Liu, Y.; He, R.; Jin, J.; Liu, C.; Chen, X. Quantifying Attribution of Runoff Change for Major Rivers in China. *Adv. Water Sci.* **2020**, *31*, 313–323. [\[CrossRef\]](#)
31. Qiao, C.; Ning, Z.; Wang, Y.; Sun, J.; Lin, Q.; Wang, G. Impact of Climate Change on Water Availability in Water Source Areas of the South-to-North Water Diversion Project in China. *Front. Earth Sci.* **2021**, *9*, 747429. [\[CrossRef\]](#)
32. Stouffer, R.J.; Eyring, V.; Meehl, G.A.; Bony, S.; Senior, C.; Stevens, B.; Taylor, K.E. Cmp5 Scientific Gaps and Recommendations for Cmp6. *Bull. Amer. Meteorol. Soc.* **2017**, *98*, 95. [\[CrossRef\]](#)
33. Zhang, S.; Chen, J. Uncertainty in Projection of Climate Extremes: A Comparison of CMIP5 and CMIP6. *J. Meteorol. Res.* **2021**, *35*, 646–662. [\[CrossRef\]](#)
34. Song, Z.; Xia, J.; She, D.; Li, L.; Hu, C.; Hong, S. Assessment of Meteorological Drought Change in the 21st Century Based on CMIP6 Multi-Model Ensemble Projections over Mainland China. *J. Hydrol.* **2021**, *601*, 126643. [\[CrossRef\]](#)
35. Zhu, H.; Jiang, Z.; Li, L. Projection of Climate Extremes in China, an Incremental Exercise from CMIP5 to CMIP6. *Sci. Bull.* **2021**, *66*, 2528–2537. [\[CrossRef\]](#)
36. Wang, G.; Zhang, J.; Xuan, Y.; Liu, J.; Jin, J.; Bao, Z.; He, R.; Liu, C.; Liu, Y.; Yan, X. Simulating the Impact of Climate Change on Runoff in a Typical River Catchment of the Loess Plateau, China. *J. Hydrometeorol.* **2013**, *14*, 1553–1561. [\[CrossRef\]](#)
37. Schewe, J.; Heinke, J.; Gerten, D.; Haddeland, I.; Arnell, N.W.; Clark, D.B.; Dankers, R.; Eisner, S.; Fekete, B.M.; Colón-González, F.J. Multimodel Assessment of Water Scarcity under Climate Change. *Proc. Natl. Acad. Sci. USA* **2014**, *111*, 3245–3250. [\[CrossRef\]](#)
38. Bao, Z.; Zhang, J.; Yan, X.; Wang, G.; Jin, J.; Liu, Y.; Guan, X. Future Streamflow Assessment in the Haihe River Basin Located in Northern China Using a Regionalized Variable Infiltration Capacity Model Based on 18 CMIP5 GCMs. *J. Water Clim. Chang.* **2020**, *11*, 1551–1569. [\[CrossRef\]](#)
39. Zhang, Y.; Su, F.; Hao, Z.; Xu, C.; Yu, Z.; Wang, L.; Tong, K. Impact of Projected Climate Change on the Hydrology in the Headwaters of the Yellow River Basin. *Hydrol. Process.* **2015**, *29*, 4379–4397. [\[CrossRef\]](#)
40. Wang, Y.; Yancg, X.; Zhang, M.; Zhang, L.; Yu, X.; Ren, L.; Liu, Y.; Jiang, S.; Yuan, F. Projected Effects of Climate Change on Future Hydrological Regimes in the Upper Yangtze River Basin, China. *Adv. Meteorol.* **2019**, *2019*, 1545746. [\[CrossRef\]](#)
41. Su, B.; Huang, J.; Zeng, X.; Gao, C.; Jiang, T. Impacts of Climate Change on Streamflow in the Upper Yangtze River Basin. *Clim. Chang.* **2017**, *141*, 533–546. [\[CrossRef\]](#)
42. Qin, P.; Liu, M.; Du, L.; Xu, H.; Liu, L.; Xiao, C. Climate Change Impact Ob Runoff in the Upper Yangtze River Basin. *Adv. Clim. Chang. Res.* **2019**, *15*, 405–415.
43. Huang, J.; Wang, Y.; Su, B.; Zhai, J. Future Climate Change and Its Impact on Runoff in the Upper Reach of Yangtze River under RCP4.5 Scenario. *Meteorol. Mon.* **2016**, *42*, 614–620.
44. Su, F.; Zhang, L.; Ou, T.; Chen, D.; Yao, T.; Tong, K.; Qi, Y. Hydrological Response to Future Climate Changes for the Major Upstream River Basins in the Tibetan Plateau. *Glob. Planet. Chang.* **2016**, *136*, 82–95. [\[CrossRef\]](#)
45. Wang, Y.; Liao, W.; Ding, Y.; Wang, X.; Jiang, Y.; Song, X.; Lei, X. Water Resource Spatiotemporal Pattern Evaluation of the Upstream Yangtze River Corresponding to Climate Changes. *Quat. Int.* **2015**, *380*, 187–196. [\[CrossRef\]](#)
46. Guan, X.; Zhang, J.; Yang, Q.; Tang, X.; Liu, C.; Jin, J.; Liu, Y.; Bao, Z.; Wang, G. Evaluation of Precipitation Products by Using Multiple Hydrological Models over the Upper Yellow River Basin, China. *Remote Sens.* **2020**, *12*, 4023. [\[CrossRef\]](#)
47. Wang, G.; Zhang, J.; Jin, J.; Liu, Y.; He, R.; Bao, Z.; Liu, C.; Li, Y. Regional Calibration of a Water Balance Model for Estimating Stream Flow in Ungauged Areas of the Yellow River Basin. *Quat. Int.* **2014**, *336*, 65–72. [\[CrossRef\]](#)
48. Kraaijenbrink, P.D.; Stigter, E.E.; Yao, T.; Immerzeel, W.W. Climate Change Decisive for Asia's Snow Meltwater Supply. *Nat. Clim. Chang.* **2021**, *11*, 591–597. [\[CrossRef\]](#)
49. Wu, J.; Gao, X. A Gridded Daily Observation Dataset over China Region and Comparison with the Other Datasets. *Chin. J. Geophys.* **2013**, *56*, 1102–1111. [\[CrossRef\]](#)
50. Wu, J.; Gao, X.; Giorgi, F.; Chen, D. Changes of Effective Temperature and Cold/Hot Days in Late Decades over China Based on a High Resolution Gridded Observation Dataset. *Int. J. Climatol.* **2017**, *37*, 788–800. [\[CrossRef\]](#)
51. Xu, Y.; Gao, X.; Shen, Y.; Xu, C.; Shi, Y.; Giorgi, F. A Daily Temperature Dataset over China and Its Application in Validating a RCM Simulation. *Adv. Atmos. Sci.* **2009**, *26*, 763–772. [\[CrossRef\]](#)
52. Song, Y.H.; Chung, E.-S.; Shahid, S. Spatiotemporal Differences and Uncertainties in Projections of Precipitation and Temperature in South Korea from CMIP6 and CMIP5 General Circulation Models. *Int. J. Climatol.* **2021**, *41*, 5899–5919. [\[CrossRef\]](#)
53. You, Q.; Cai, Z.; Wu, F.; Jiang, Z.; Pepin, N.; Shen, S.S.P. Temperature Dataset of CMIP6 Models over China: Evaluation, Trend and Uncertainty. *Clim. Dyn.* **2021**, *57*, 17–35. [\[CrossRef\]](#)
54. Wang, L.; Zhang, J.; Shu, Z.; Wang, Y.; Bao, Z.; Liu, C.; Zhou, X.; Wang, G. Evaluation of the Ability of CMIP6 Global Climate Models to Simulate Precipitation in the Yellow River Basin, China. *Front. Earth Sci.* **2021**, *9*, 751974. [\[CrossRef\]](#)
55. Fang, G.; Yang, J.; Chen, Y.; Li, Z.; De Maeyer, P. Impact of GCM Structure Uncertainty on Hydrological Processes in an Arid Area of China. *Hydrol. Res.* **2018**, *49*, 893–907. [\[CrossRef\]](#)

56. Yang, X.; Zheng, W.; Ren, L.; Zhang, M.; Wang, Y.; Liu, Y.; Yuan, F.; Jiang, S. Potential Impact of Climate Change to the Future Streamflow of Yellow River Basin Based on CMIP5 Data. *Proc. IAHS* **2018**, *376*, 97–104. [\[CrossRef\]](#)
57. Hassan, Z.; Shamsudin, S.; Harun, S. Application of SDSM and LARS-WG for Simulating and Downscaling of Rainfall and Temperature. *Theor. Appl. Climatol.* **2014**, *116*, 243–257. [\[CrossRef\]](#)
58. IPCC. *Climate Change 2021: The Physical Science Basis*; Cambridge University Press: Cambridge, UK, 2021.
59. Labat, D.; Godderis, Y.; Probst, J.L.; Guyot, J.L. Evidence for Global Runoff Increase Related to Climate Warming. *Adv. Water Resour.* **2004**, *27*, 631–642. [\[CrossRef\]](#)
60. Liu, J.; Wang, J.; Jiao, M.; Zhang, R. Response of Water Resources in the Yellow River Basin to Global Climate Change. *Arid Zone Res.* **2011**, *28*, 860–865. [\[CrossRef\]](#)
61. Wang, G.; Qiao, C.; Liu, M.; Du, F.; Ye, T.; Wang, J. The future water resources regime of the Yellow River basin in the context of climate change. *Hydro-Sci. Eng.* **2020**, *2*, 1–8. [\[CrossRef\]](#)
62. Yan, Z.; Zhou, Z.; Liu, J.; Wang, H.; Li, D. Water Use Characteristics and Impact Factors in the Yellow River Basin, China. *Water Int.* **2020**, *45*, 148–168. [\[CrossRef\]](#)
63. Chen, J.; He, D.; Cui, S. The Response of River Water Quality and Quantity to the Development of Irrigated Agriculture in the Last 4 Decades in the Yellow River Basin, China. *Water Resour. Res.* **2003**, *39*, WR01234. [\[CrossRef\]](#)
64. Peng, S.; Zheng, X.; Wang, Y.; Jiang, G. Study on Water-Energy-Food Collaborative Optimization for Yellow River Basin. *Adv. Water Sci.* **2017**, *28*, 681–690. [\[CrossRef\]](#)
65. Zhang, J.; Chen, L.; Li, B.; Xu, W. Research on the precipitation of precipitation change with in Upper Yangtze River Basin during 2011–2060. *Water Resour. Hydropower Eng.* **2012**, *43*, 4–9. [\[CrossRef\]](#)
66. Yang, X.; Yu, X.; Wang, Y.; Liu, Y.; Zhang, M.; Ren, L.; Yuan, F.; Jiang, S. Estimating the Response of Hydrological Regimes to Future Projections of Precipitation and Temperature over the Upper Yangtze River. *Atmos. Res.* **2019**, *230*, 104627. [\[CrossRef\]](#)
67. Zhao, Q.; Ding, Y.; Wang, J.; Gao, H.; Zhang, S.; Zhao, C.; Xu, J.; Han, H.; Shangguan, D. Projecting Climate Change Impacts on Hydrological Processes on the Tibetan Plateau with Model Calibration against the Glacier Inventory Data and Observed Streamflow. *J. Hydrol.* **2019**, *573*, 60–81. [\[CrossRef\]](#)
68. Xu, W.; Chen, J.; Gu, L.; Zhu, B.; Zhuan, M. Runoff Response to 1.5 °C and 2.0 °C Global Warming for the Yangtze River Basin. *Adv. Clim. Chang. Res.* **2020**, *16*, 690–705.
69. Li, K. *Study on the Evolution Law and Future Trend of Runoff in the Three-River Headwater Region*; Changjiang River Scientific Research Institute: Wuhan, China, 2021.
70. Mujumdar, P.P.; Ghosh, S. Modeling GCM and Scenario Uncertainty Using a Possibilistic Approach: Application to the Mahanadi River, India. *Water Resour. Res.* **2008**, *44*, W06407. [\[CrossRef\]](#)
71. Gao, J.; Sheshukov, A.Y.; Yen, H.; Douglas-Mankin, K.R.; White, M.J.; Arnold, J.G. Uncertainty of Hydrologic Processes Caused by Bias-Corrected CMIP5 Climate Change Projections with Alternative Historical Data Sources. *J. Hydrol.* **2019**, *568*, 551–561. [\[CrossRef\]](#)
72. Janzwood, S. Confident, Likely, or Both? The Implementation of the Uncertainty Language Framework in IPCC Special Reports. *Clim. Chang.* **2020**, *162*, 1655–1675. [\[CrossRef\]](#)
73. Vetter, T.; Reinhardt, J.; Floerke, M.; van Griensven, A.; Hattermann, F.; Huang, S.; Koch, H.; Pechlivanidis, I.G.; Ploetner, S.; Seidou, O.; et al. Evaluation of Sources of Uncertainty in Projected Hydrological Changes under Climate Change in 12 Large-Scale River Basins. *Clim. Chang.* **2017**, *141*, 419–433. [\[CrossRef\]](#)
74. Bao, X.; Zhang, F. Evaluation of NCEP-CFSR, NCEP-NCAR, ERA-Interim, and ERA-40 Reanalysis Datasets against Independent Sounding Observations over the Tibetan Plateau. *J. Clim.* **2013**, *26*, 206–214. [\[CrossRef\]](#)
75. Korkanc, S.Y. Impacts of Recreational Human Trampling on Selected Soil and Vegetation Properties of Aladag Natural Park, Turkey. *Catena* **2014**, *113*, 219–225. [\[CrossRef\]](#)
76. Ren, Z.; Zhu, L.; Wang, B.; Cheng, S. Soil Hydraulic Conductivity as Affected by Vegetation Restoration Age on the Loess Plateau, China. *J. Arid Land* **2016**, *8*, 546–555. [\[CrossRef\]](#)
77. Wang, H.; Sun, F. Variability of Annual Sediment Load and Runoff in the Yellow River for the Last 100 Years (1919–2018). *Sci. Total Environ.* **2021**, *758*, 143715. [\[CrossRef\]](#)
78. Jiang, W.; Yuan, L.; Wang, W.; Cao, R.; Zhang, Y.; Shen, W. Spatio-Temporal Analysis of Vegetation Variation in the Yellow River Basin. *Ecol. Indic.* **2015**, *51*, 117–126. [\[CrossRef\]](#)
79. Xu, X.; Yang, D.; Yang, H.; Lei, H. Attribution Analysis Based on the Budyko Hypothesis for Detecting the Dominant Cause of Runoff Decline in Haihe Basin. *J. Hydrol.* **2014**, *510*, 530–540. [\[CrossRef\]](#)
80. Poulin, A.; Brissette, F.; Leconte, R.; Arseneault, R.; Malo, J.-S. Uncertainty of Hydrological Modelling in Climate Change Impact Studies in a Canadian, Snow-Dominated River Basin. *J. Hydrol.* **2011**, *409*, 626–636. [\[CrossRef\]](#)
81. Zhang, L.; Su, F.; Yang, D.; Hao, Z.; Tong, K. Discharge Regime and Simulation for the Upstream of Major Rivers over Tibetan Plateau. *J. Geophys. Res. Atmos.* **2013**, *118*, 8500–8518. [\[CrossRef\]](#)
82. Mukhopadhyay, B.; Khan, A. A Reevaluation of the Snowmelt and Glacial Melt in River Flows within Upper Indus Basin and Its Significance in a Changing Climate. *J. Hydrol.* **2015**, *527*, 119–132. [\[CrossRef\]](#)
83. Chu, D. Spatiotemporal Variability of Snow Cover on Tibet, China Using MODIS Remote-Sensing Data. *Int. J. Remote Sens.* **2018**, *39*, 6784–6804. [\[CrossRef\]](#)

-
84. Yi, S.; Song, C.; Heki, K.; Kang, S.; Wang, Q.; Chang, L. Satellite-Observed Monthly Glacier and Snow Mass Changes in Southeast Tibet: Implication for Substantial Meltwater Contribution to the Brahmaputra. *Cryosphere* **2020**, *14*, 2267–2281. [[CrossRef](#)]
 85. Grigg, N.S. Large-Scale Water Development in the United States: TVA and the California State Water Project. *Int. J. Water Resour. Dev.* **2021**, 1–19, Online. [[CrossRef](#)]
 86. Ren, S.; Kingsford, R.T. Modelling Impacts of Regulation on Flows to the Lowbidgee Floodplain of the Murrumbidgee River, Australia. *J. Hydrol.* **2014**, *519*, 1660–1667. [[CrossRef](#)]